New Simplified Lymphoscintigraphic Technique in Patients with Breast Cancer

Shoji Terui and Hiroshi Yamamoto

Division of Nuclear Medicine and Surgery, National Cancer Center Hospital, Tokyo, Japan

To achieve the visualization of regional lymph nodes using lymphoscintigraphy, 100 pre-operative patients with breast cancer were studied, with [^{99m}Tc]rhenium colloid having been injected into the periosteum of their ribs. In order to identify the exact location of the visualized nodes, the obtained lymphoscintigram was superimposed onto the patient's chest roentgenogram. The visibility of the internal mammary region was 91% on the affected side, and 93% on the healthy side, whereas the visibility of the axillary region was 85% and 86%, respectively. The injection resulted in simultaneous visualization of both the internal mammary and the axillary nodes: in our series, it meant the visualization of 82 patients (82%) on the affected side and 83 patients (83%) on the healthy side. Our technique appears to be a rather efficient method for imaging the regional lymph nodes in breast cancer patients.

J Nucl Med 30:1198–1204, 1989

Lymphoscintigraphy is a simple and noninvasive examination designed to help us see the regional lymph nodes of a cancer-affected patient. Rosenblum and Hill demonstrated the presence of both the axillary and the internal mammary nodes by using technetium-99m (^{99m}Tc) sulfide colloid first for subcostal and then for areolar injections (*1,2*). Mclean did the same thing for the subcostal and interdigital injections, respectively (*3*). Hultborn and associates, with the aid of radioactive colloidal gold, showed the way a lymph drainage spreads from every quadrant of the breast to both the axillary and the internal mammary lymph nodes (*4*). As is well known, some of the lymph from the mammary glands is transported by the lymphatics that go through the pectoralis major muscle and the intercostal spaces and then run along and amid the internal mammary vessels (*5*). It is here in the lymphatic system that we apply our method whose aim is to achieve the most effective visualization of the respective regional lymph nodes. In order to identify the exact location of these lymph nodes, we inject [^{99m}Tc]rhenium colloid (to be more fully explained below), superimposing the obtained image (lymphoscintigram) on the patient's chest roentgenogram (*6*). In such a superimposed image, we evaluated tumor spread.

Received July 22, 1988; revision accepted Apr. 6, 1989.

For reprints contact: Shoji Terui, MD, Div. of Nuclear Medicine, National Cancer Center Hospital, 5-1-1 Tsukiji, Chuo-ku, Tokyo 104.

MATERIALS AND METHODS

From January 1985 to June 1987, at our National Cancer Center Hospital in Tokyo, 100 pre-operative patients with breast cancer were examined according to the new lymphoscintigraphic method. Of these 100 patients, 48 were subsequently subjected to the excision of the internal mammary lymph nodes. The location of the tumor and the clinical stage of the patients are classified according to the UICC Classification (*7*) and are summarized in Table 1. To obtain our lymphoscintigram, we used the above-mentioned [^{99m}Tc]rhenium colloid (*8*). Although the injection technique of [^{99m}Tc]Re appears to be rather simple, the interdependence of each step of the technique is essential to the procedure and, therefore, steps should be followed closely (*6*). On the day before the projected surgery, a total of 10 mCi of [^{99m}Tc]Re in 2 ml is injected into the periosteum in the following way: while exerting pressure on the skin of the rib with one's free hand, a 23-gauge, 1.25-in. needle is pushed vertically into the skin, first on the fourth rib, always in the direction of the midclavicular line, that is medial to this line. The needle traverses the mammary glands and the pectoralis muscles to reach the middle of the respective rib; here 0.5 ml of [^{99m}Tc]Re is then injected. The same procedure is followed for the fifth rib. If, however, the tumor has been perceived as closer to the midclavicular line, we inject [^{99m}Tc]Re between the tumor and the sternum, that is, if the tumor is in the upper inner quadrant; if, however, it is in the upper outer quadrant, we inject medial to the midclavicular line. In either case, a similar injection is given to the fourth and fifth ribs in the direction of the midclavicular line in the healthy breast. This procedure always causes some unavoidable pain, but the procedure is completed in <1 min.

TABLE 1
Location of the Tumor and Clinical Stages of 100 Patients

	No. of Patients	Clinical stage				
		I	II	IIIA	IIIB	Unstaged
Upper-inner quadrant	(28)	8	16	2	1	1
Lower-inner quadrant	(8)	3	3	2	0	0
Upper-outer quadrant	(34)	6	18	6	2	2
Lower-outer quadrant	(5)	2	3	0	0	0
Central portion	(15)	0	10	1	3	1
Unknown	(10)	4	4	0	0	2
Total	(100)	23	54	11	6	6

Lymphoscintigraphic images are taken in the following way: 3 hr after the injections, an anterior-view-lymphoscintigram is obtained on the 35 × 43 cm film (KODAK T-Mat G Film) with a large field gamma camera. The collimator is of the low-energy, parallel hole type and results in at least 1,300,000 counts per image. The injection sites are covered with leaden plates because of high radioactivity. The sternal notch is marked mechanically by a technician. The technical apparatus used sounds complicated, but with practice is reduced to the following concrete procedure. The patient lay under the gamma camera; the radioactive pointer in the hand of the surgeon then localizes the patient's sternal notch, which at the same time is automatically marked on the lymphoscintigraphic film; in this way we are able to obtain a realistic life-sized lymphoscintigram (Fig. 1). This life-sized lymphoscintigram is then superimposed upon the previously taken postero-antero chest roentgenogram with the patient in the upright position—the ribs, clavicles, and the contours of the breasts are marked with inerasable ink onto the lymphoscintigram (Fig. 2) thus obtaining what may be called a superimposed image (SI) (Fig. 3). By this SI, the regions of the visualized (hot) nodes are easily assessed as belonging to anatomic groups such as axillary (low, middle), axillary apex, infraclavicular (referred to as levels I, II, and III, respectively), and intercostal spaces (*9*). Terminology concerning the so-called intercostal space is not yet unified; in this paper we understand it surgically as, for example, first, second, third one, and so on, with its adjacent space, excluding only the rib coming next; thus, from the point of view of surgery, the first intercostal space would mean the nodes of the first rib encompassing also the intervening intercostal space between the first and second rib. On the other hand, concerning those levels on the SI, we have found it useful to call level I the lower part of the second rib, level II that between the first and the second rib, and level III the upper part of the first rib.

After the regions of the visualized (hot) nodes have been assessed, we proceed to count them.

Following the operation, the lymph nodes are dissected from the specimens and divided into the anatomic groups above-mentioned which are then mapped on the appropriate paper and given running numbers.

Of the 100 cases, the 48 specimens of the regional lymph nodes were examined scintigraphically once more under the gamma camera as to their actual hot spots (Fig. 4). The dissected nodes were then studied histologically, and correlated with the visualized ones.

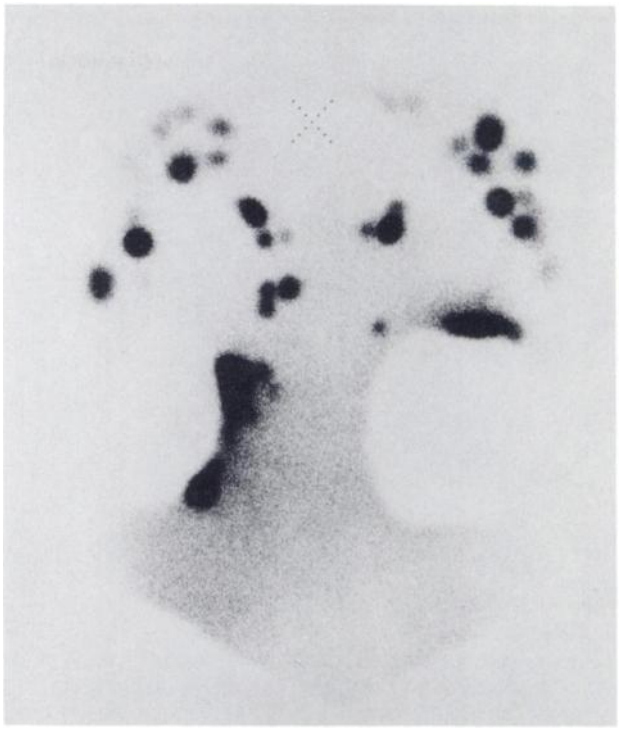

FIGURE 1
A life-sized lymphoscintigram taken with the 35 × 43 cm film. The tumor was located in the left lower-outer quadrant (T1N1M0). Many hot nodes were noticed in the image. White round spots are injection sites covered with leaden plates. The sternal notch is marked on the lymphoscintigram (x).

RESULTS

The visibility of the internal mammary region is 91% (91/100) in the affected side and 93% (93/100) in the healthy side, whereas the visibility of the axillary region is 85% (85/100) and 86% (86/100), respectively (Table 2). The injection of the [^{99m}Tc]Re into the periosteum of the ribs results in a fairly extensive simultaneous visualization of both the internal mammary nodes and the axillary ones: in our case, it visualized 82 patients (82%) on the affected side and 83 patients (83%) on the healthy side. The number of patients who showed no lymph nodes on the affected side was six, on the healthy side four. Thus, the total of ten patients could not be visualized as to their lymph nodes. Of these ten patients, only two patients, however, could not be visualized at all on the SI either as to their healthy lymph nodes or the involved ones; one of these patients belonged to the clinical stage I, and the other to the clinical stage II. This might have been the result of defective labeling of ^{99m}Tc.

A total of 600 lymph nodes were visualized in both

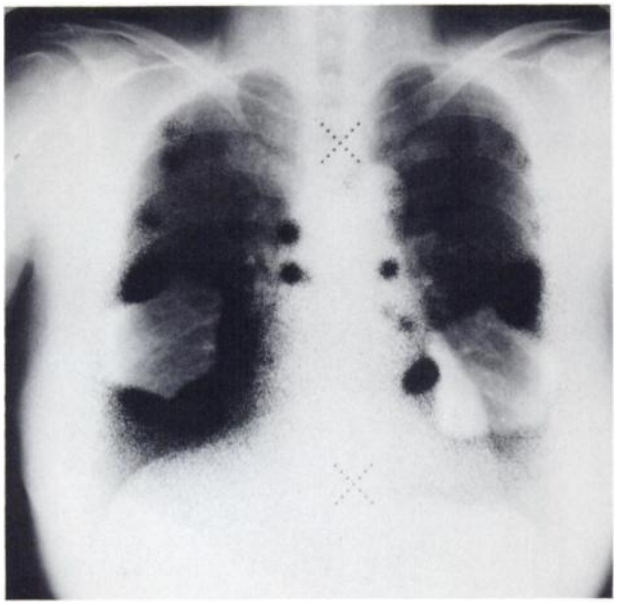

FIGURE 2
The life-sized lymphoscintigram superimposed upon the patient's chest roentgenogram. The roentgen image of an object is larger than the object itself, because of the divergence of the x-rays. There appears, with our method of procedure, only a negligible difference between the life-sized lymphoscintigram and the chest roentgen image, thus enhancing an almost exact location.

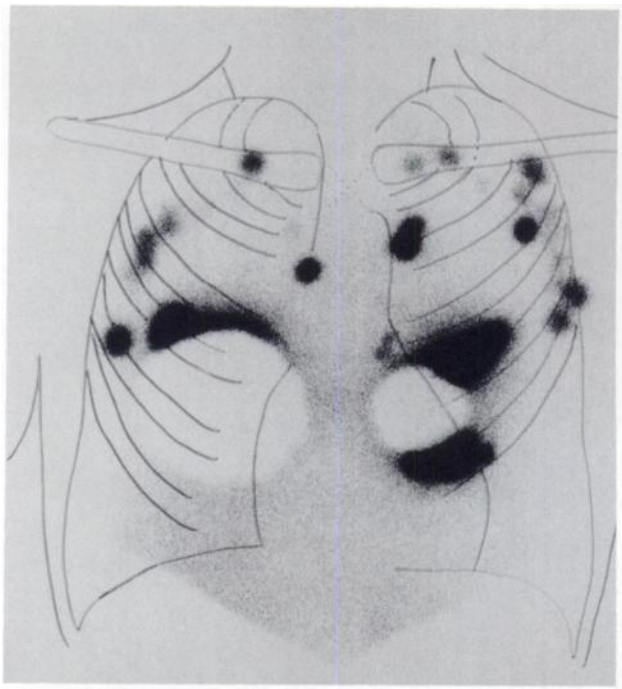

FIGURE 3
A superimposed image. The tumor is 4 × 3.5 cm in size and located in the lower-outer quadrant of the right breast (T2N0M0). One hot internal mammary node was noticed in the second intercostal space and five nodes in the axillary region of the affected side. Of these five nodes, we diagnosed one node to be on the level III and four nodes on the level I. No difference was detected concerning the number and the visibility of the nodes both on the healthy side and the affected one. By the way, it is not easy to diagnose the existence of the lymph nodes in both the third and fourth intercostal space because of the leaden plates, necessarily imposed for safety.

the left and the right internal mammary region (average six nodes per patient and within the range of from 1 to 8, Table 3). There were 287 nodes in the affected side (average 2.9 nodes per person) and 313 (average 3.1 nodes) in the healthy side. The visualized nodes could be seen spreading from the infraclavicular right down to the fifth intercostal space. The best visualized region of the internal mammary nodes is the second intercostal space. Compared with the internal mammary nodes, a grand total of 567 nodes could be visualized in the axillary region (average 5.7 nodes per patient and within the range of 1 to 11).

Figure 5 shows the visibility of regions of the anatomic groups according to their clinical stages. The visibility of the stages I, II, and IIIA reveals the same pattern and also there is no difference in visibility between the healthy side and the affected one. Intercostal spaces of the first and second ribs showed a higher visibility than those of the third and fourth ribs. However, according to our examination, the visibility of the stage IIIB was remarkably decreased to only 33% for the intercostal spaces of the first, second, and third ribs, respectively. It was also only 16.7% for the levels I, II, and III, respectively.

Table 4 summarizes the number of the visualized nodes on the SI, the number of the dissected nodes (of the specimen), and the number of the visualized nodes on the scintigram of a pertinent specimen. As to the internal mammary region, a total of 242 nodes were removed operationally from the internal mammary region and as many as 152 (62.8%) nodes could be observed visually on the scintigram of the postsurgical specimen. By comparison, 126 (52.1%) nodes had been visualized on the SI pre-surgically. The number of the visualized nodes of the pertinent specimen was greater than that of the SI except for the second intercostal space.

Speaking of the axillary region, on the other hand, a total of 1,026 nodes were removed operationally from the axillary region, but only 87 (8.5%) nodes could be visualized on the scintigram of the specimen. The number of the visualized nodes of the pertinent specimen was less than that of the pre-surgical SI. The visibility of the levels I, II, and III was 6.9% (48/691), 10.2% (29/284), and 19.6% (10/51), respectively. Histologically, there was no lymph node metastasis with Stage I patients. In the stage II patients, metastases were only found in the axillary region.

Concerning the stage-III patients, a total of 84 nodes were removed surgically from the internal mammary region of 15 patients (Table 5). Histologically metas-

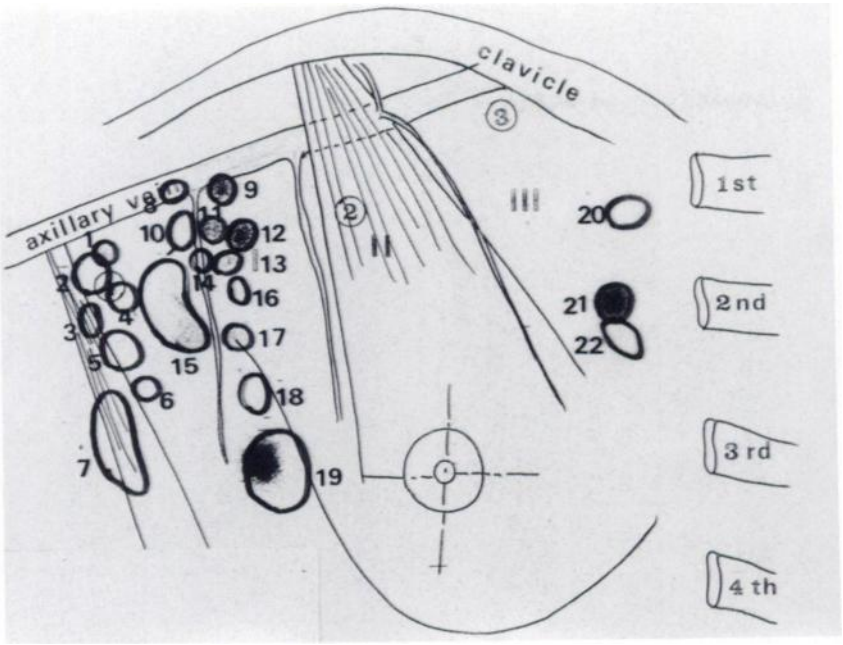

FIGURE 4
A scintigram of the specimen of the Figure 3 patient. The scintigram of the specimen was superimposed upon the sheet of paper with anatomical schema on which the dissected nodes had been mapped after the operation. By this method, the hot nodes are easily assessed as belonging to anatomical groups. The total of 22 nodes were dissected; there were 19 nodes of the level I and three nodes of the internal mammary region. One hot node in the internal mammary region (No. 21) and six nodes on the level I (Nos. 9, 11, 12, 13, 15, and 19) were visualized as hot on the scintigram. Histologically, four nodes (Nos. 12, 16, 17, and 19) were found with cancer.

tases were found in 13 out of 84 nodes (15.5%). Forty-four nodes out of 84 (52.4%) could be observed visually on the scintigram; 40 nodes (47.6%), however, could not. Three of 44 nodes (6.8%) were visualized as hot nodes with cancer. Ten of those 40 (25.0%) nonvisualized, so-called cold nodes, had metastasis. On the other hand, a total of 335 nodes were removed from the axillary region. Only 26 nodes out of 369 (7.8%) could be observed visually on the scintigram. The percentile visibility of cancerous lymph nodes of the levels I, II, and III amounted to 25%, 44.4%, and 20%, respectively. One hundred forty-five of those 369 (46.9%) nonvisualized nodes had metastasis.

DISCUSSION

To obtain a simultaneous visualization of the internal mammary and the axillary nodes using lymphoscintigraphy, the combination of the subcostal and areolar injections as well as the subcostal and interdigital injections have been tried (*1–3*). In our experience, radioactive colloid should be injected near the primary site of the tumor where it will then follow the same pathway taken by the metastatic process itself. The protuberant breast extends from the second or third rib to the sixth or seventh costal cartilage (*10*); we inject the fourth and the fifth rib periosteum located in the very middle of the breast; in this way, the radioactive colloid spreads simultaneously both to the internal mammary nodes and the axillary ones (Fig. 3), with simultaneous visualization of both the internal mammary and the axillary nodes reaching 82% (82/100) on the affected side and 83% (83/100) on the healthy side, respectively (Table 2). Concerning the internal mammary region only, its visibility was 91% on the affected side and 93% on the healthy side. The visibility of the internal mammary region was the same as that obtained by Ege (*11*).

TABLE 2
Visibility of the Internal Mammary and Axillary Regions of 100 Patients

	Affected side	Healthy side
Internal mammary region	91	93
Axillary region	85	86
Internal mammary and axillary region simultaneously	82	83
No lymph node visualized	6	4

TABLE 3
Number of Visualized Nodes in the Internal Mammary and Axillary Region on the Superimposed Image

	Affected side	Healthy side	Total
Internal mammary region			
Intercostal space			
First	98	99	197
Second	121	134	255
Third	54	56	110
Fourth	14	14	28
Fifth	0	10	10
Total	287	313	600
Axillary region			
Level I	175	155	330
Level II	88	102	190
Level III	23	24	47
Total	286	281	567

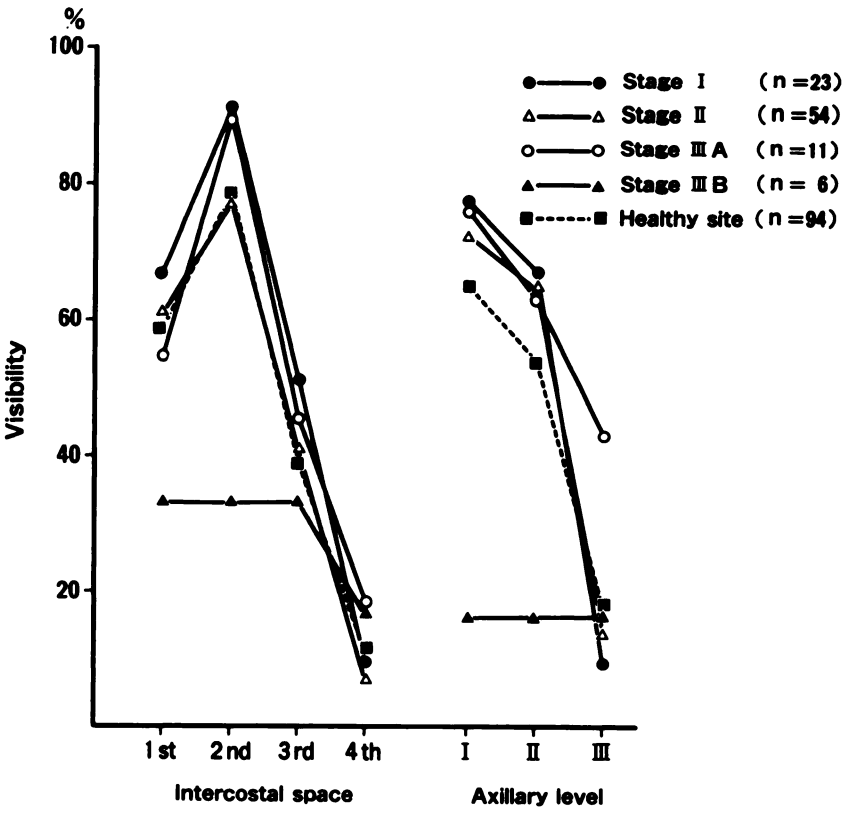

FIGURE 5
The visibility of the healthy side of the first, second, third, and fourth intercostal space was 59%, 78%, 39%, and 11%, respectively. Also the visibility of the levels I, II, and III was 65%, 54%, and 18%, respectively. The visibility of the stages I, II, and IIIA shows the same pattern as that of the healthy side. However, the visibility of the stage IIIB appears to be remarkably decreased in both the intercostal spaces and the axillary region, because of a cancerous invasion of the lymphatic system.

However, we were not able to image as many as six internal mammary nodes per patients (Table 3). Many investigators have reported that they have seen as many as 12 internal mammary nodes per patient (*11–16*). In our injection technique, the visibility of the third and fourth intercostal space was less than that of first and second ones, because of the deposition of the radioactivity in the injected sites (Fig. 3).

The axillary nodes visualized by our method spread to levels I, II, and III of the axillary region (Table 3, 4). Comparing this with the visualization of axillary nodes obtained by both the areolar and the interdigital injection (*1–3*), these visualized nodes would be identified as spreading mostly to level I of the axillary region. Of course, all of these levels are difficult areas to diagnose both as to the existence and the extent of the lymph nodes in question.

On the negative side, there was a difference between the SI and the scintigram of the specimens concerning the number of the visualized nodes (Table 4). As to the internal mammary region, the number of the visualized nodes on the pertinent specimen was greater than that of the SI. On the other hand, it was reversed for the axillary region. This discrepancy is because of the fact that one hot node may sometimes cover two or more nodes, and vice versa. Or it may be that the dissected nodes (especially tiny ones) were overlooked by the surgeon and were not mapped out adequately.

Many papers have been published on the usefulness of lymphoscintigraphy in breast cancer (*1–4,11,12,14, 17*). Relying on photographs, these reports only show the accumulation of radioactive colloid in the form of hot spots against a crudely sketched, handdrawn anatomic background. The reason is clear: it has always been difficult to diagnose the exact location of those lymph nodes. Thus Sirr used a video imaging system

TABLE 4
Correlation of the Numbers of Lymph Nodes Visualized on the SI and of the Dissected Nodes of 48 Patients

	Intercostal space					Level			
	First	Second	Third	Fourth	(Total)	I	II	III	(Total)
Total no. of dissected nodes	75	83	62	22	(242)	691	284	51	(1026)
Hot nodes of the pertinent specimen	50	51	37	14	(152)	48	29	10	(87)
Visualized nodes on the SI	36	57	26	7	(126)	83	44	13	(140)

TABLE 5
Results of the Lymph Node Metastases of the Stage III Patients

	Internal mammary nodes					Axillary nodes			
	First	Second	Third	Fourth	(Total)	I	II	III	(Total)
Total no. of lymph node dissected	25	34	20	6	(84)	197	108	30	(335)
Visualized on the scintigram	14	20	7	3	(44)	12	9	5	(26)
Histologically found with cancer	1	1	1	0	(3)	3	4	1	(8)
Impossible to visualize on the scintigram	10	14	13	3	(40)	185	99	25	(309)
Histologically found with cancer	1	3	4	2	(10)	84	49	12	(145)

and superimposed chest radiographs as well as aerosol ventillation scans (*18*). By such a superimposing method, he was able to show a precise anatomic distribution of functional abnormality. Our SI method of superimposing a life-sized lymphoscintigram on a chest roentgenogram reveals the exact location of the lymph nodes against the anatomic background of the structures (Fig. 2). Such images are easy to produce and easy to grasp as to the spread and exact location of the visualized lymph nodes (Fig. 3). Of course, the roentgen image of an object is larger than the real object, because of the divergence of the roentgen rays (*19*). To find the true object dimension, the image dimension is multiplied by a correction factor. In our 100-case history, there has been only a negligible difference between the life-sized lymphoscintigram and the chest roentgen image, thus enhancing the exactness of the location.

Our injection technique in conjunction with the SI provides a rather efficient and easily manageable method for imaging the regional lymph nodes of breast cancer patients. Besides, the SI may be applied to determine the exact field for radiation therapy (*20,21*).

Lymph nodes with cancerous invasion are usually depicted as cold. We may add one more interesting fact concerning the probability of lymph node metastases in those visualized nodes of the stage-III patients: the visibility of the axillary region is low but there is a higher tendency to visualize nodes involved with cancer compared with the frequency obtained in the internal mammary region (Table 5). We as yet cannot explain why the axillary nodes of those stage-III patients have shown such a high percentage of visualized nodes with cancer compared with the nodes of the stage I and stage II patients. We will have to study systematically many more patients in this respect.

As for the identification of lymph node metastases with hot nodes on the lymphoscintigram, it is our hypothesis that a radionuclide labeled with a monoclonal antibody promises to be of special clinical value (*22–24*). Our use of the lymphoscintigraphy to diagnose the spread of the cancer in a lymph node constitutes a normative model of a highly manageable usefulness: the radionuclide with a monoclonal antibody near the primary site of the tumor runs along the metastasis of the cancer cell itself. But more research on this line is at present blocked by the fact that necessary materials for research and surgery are not available.

REFERENCES

1. Rosenblum I, Wischnitzer T, Stadler JA, et al. Lymphography of the breast as an accessory in the early diagnosis and detection of carcinoma of the breast: lymphography as a prognostic tool. *World J Surg* 1982; 6:126–129.
2. Hill NS, Ege GN, Greyson ND, et al. Predicting nodal metastases in breast cancer by lymphoscintigraphy. *Can J Surg* 1983; 26:507–509.
3. Mclean RG, Ege GN. Prognostic value of axillary lymphoscintigraphy in breast carcinoma patients. *J Nucl Med* 1986; 27:1116–1124.
4. Hultborn KA, Larsson LG, Ragnhult I. The lymph drainage from the breast to the axillary and parasternal lymph nodes, studied with the aid of colloidal Au-198. *Acta Radiol* 1955; 43:52–64.
5. Stiles HJ. Contributions to the surgical anatomy of the breast and axillary lymphatic glands. *Edinburgh Med J* 1982; 37: 1099–1112.
6. Terui S, Taira N, Nanasawa T, et al. Lymphoscintigram in breast cancer: a superimposed technique. In: *New frontiers in mammary pathology 1986*. Boston/ Dordrecht/Lancaster: Martinus Nijhoff Publishers, 1986:403–410.
7. Spiessl B, Hermanek P, Scheibe O, et al. TNM-Atlas. Illustrated guide to the TNM/pTNM-classification of malignant tumors. Berlin, Heidelberg, New York: Springer-Verlag, 1982.
8. Pecking A. Resultats preliminaires de l'essai d'un nouveau compose pour lymphographies isotopiques: Le sulfure de rhenium colloida marque par du technetium-99m. *J Fr Biophys Med Nucl* 1978; 2:117–120.
9. Beahrs OH, Mywea MH. Manual for staging of cancer. Philadelphia: J.B. Lippincott, 1983.
10. Haagensen CD. Disease of the breast. Philadelphia, London, Toronto, W.B. Saunders, 1971:1–2.
11. Ege GN. Internal mammary lymphoscintigraphy. The rationale, technique, interpretation and clinical application: a review based on 848 cases. *Radiology* 1976; 118:101–107.

12. Schenck P. Szintigraphische Darstellung des parasternalen Lymphsystems. Strahlentherapie 1966; 130: 504–508.
13. Manji MF. Internal mammary lymphoscintigraphy in breast carcinoma: possible significance in relation to current treatment. *J De L'association Candienne Radiol* 1982; 33:10–14.
14. Stibbe EP. The internal mammary lymphatic glands. *J Anat* 1918; 52:257–264.
15. McDonald JJ, Haagensen CD, Stout AP. Metastasis from mammary carcinoma to the supraclavicular and internal mammary lymph nodes. *Surgery* 1953; 34: 521–542.
16. Soerensen B. Recherches sur la localisation des ganglions lymphatignes parastenaux, par rapport aux espares intercostaux. *J Internat de Chir* 1951; 11:501–509.
17. Ege GN. Internal mammary lymphoscintigraphy: a rational adjunct to the staging and management of breast carcinoma. *Clin Radiol* 1978; 29:453–456.
18. Sirr SA, Elliott GR, Regelmann WE, et al. Aerosol penetration ratio: a new index of ventilation. *J Nucl Med* 1986; 27:1343–1346.
19. Lusted LB, Keats TE. Atlas of roentgenographic measurement, 2nd ed. Chicago: Year Book of Medical Publishers Inc., 1967:13.
20. Rose CM, Kaplan WD, Marck A, et al. Parasternal lymphoscintigraphy-implications for treatment planning of internal mammary lymph nodes in breast cancer. *Int J Radiol Oncol Biol Phys* 1979; 5:1849–1853.
21. Robert RS, Lee MC, Robert EZ. Utilization of parasternal lymphoscintigraphy in radiation therapy of breast carcinoma. *Int J Radiol Oncol Biol Phys* 1982; 8:1059–1063.
22. Weinstein JN, Steller MA, Covell DG, et al. Monoclonal antitumor antibodies in the lymphatics. *Cancer Treat Rep* 1984; 68:257–264.
23. Nelp WB, Eary JF, Jones RF, et al. Preliminary studies of monoclonal antibody lymphoscintigraphy in malignant melanoma. *J Nucl Med* 1987; 28:34–41.
24. Keenan AM, Weinstein JN, Mulshine JL, et al. Immunolymphoscintigraphy in patients with lymphoma after subcutaneous injection of indium-111-labeled T101 monoclonal antibody. *J Nucl Med* 1987; 28:42–46.